

CURRENT TRANSPORT IN W AND WSi_x OHMIC CONTACTS TO INGAN AND INN

C.B. Vartuli, S.J. Pearton, C.R. Abernathy, J.D. MacKenzie, Dept of MSE, University of Florida, Gainesville FL; M.L. Lovejoy, R.J. Shul, J.C. Zolper, Sandia National Laboratories, Albuquerque NM; A.G. Baca Sandia National Laboratories, Compound Semiconductor Materials and Processes, Albuquerque NM; M. Hagerott-Crawford Sandia National Laboratories, Department of Photonics Research, Albuquerque NM; K.A. Jones, Army Research Laboratory, Ft. Monmouth NJ; F. Ren, Bell Laboratories, Lucent Technologies, Murray Hill NJ.

CONF-970302-24

ABSTRACT

The temperature dependence of the specific contact resistance of W and $WSi_{0.44}$ contacts on n^+ $In_{0.65}Ga_{0.35}N$ and InN was measured in the range -50 °C to 125 °C. The results were compared to theoretical values for different conduction mechanisms, to further elucidate the conduction mechanism in these contact structures. The data indicates the conduction mechanism is field emission for these contact schemes for all but as-deposited metal to InN where thermionic emission appears to be the dominant mechanism. The contacts were found to produce low specific resistance ohmic contacts to InGaN at room temperature, $Q_c \sim 10^{-7} \Omega \cdot \text{cm}^2$ for W and Q_c of $4 \times 10^{-7} \Omega \cdot \text{cm}^2$ for WSi_x . InN metallized with W produced ohmic contacts with $Q_c \sim 10^{-7} \Omega \cdot \text{cm}^2$ and $Q_c \sim 10^{-6} \Omega \cdot \text{cm}^2$ for WSi_x at room temperature.

INTRODUCTION

It has proven difficult to produce low resistance ohmic contacts to the III-nitride materials because of their wide bandgaps.¹⁻¹¹ To date little work has been done regarding the conduction mechanism in ohmic contacts to the nitrides. We would like to establish a high temperature contact technology for the nitrides, for applications such as electronics capable of operation at ≥ 500 °C, or for power switching. Cole et. al. reported that W produced contact resistivities of $\sim 10^{-4} \Omega \cdot \text{cm}^2$ on n^+ GaN, and was stable for annealing temperatures up to ~ 1000 °C. In particular the use of lower bandgap In-containing nitrides should be able to reduce the contact resistance on GaN, in analogy to the situation for $In_xGa_{1-x}As$ on GaAs.

In this paper we report the results of W and $WSi_{0.44}$ contacts deposited on n^+ $In_{0.65}Ga_{0.35}N$ and n^+ InN. Temperature dependent transmission line measurements (TLM) in the range -50 °C to 125 °C were used to obtain information about the conduction mechanism in these contact structures. Room temperature TLM measurements were also measured as a function of annealing temperature, in order to establish the stability of the contacts. A key feature of using In-based nitrides is the trade-off between contact resistance and thermal stability.

EXPERIMENTAL

The 2000 Å thick InN and InGaN samples were grown using Metal Organic Molecular Beam Epitaxy (MO-MBE) on semi-insulating, (100) GaAs substrates in an Intevac Gen II system as described previously.^{12,13} The InN and $In_{0.65}Ga_{0.35}N$ were highly autodoped n-type ($\sim 10^{20} \text{ cm}^{-3}$, and $\sim 10^{19} \text{ cm}^{-3}$ respectively) due to the presence of the native defects endemic to these materials. The samples were rinsed in $H_2O:NH_4OH$ (20:1) for 1 min just prior to deposition of the metal to remove native oxides. The metal contacts were sputter deposited to a thickness of 1000 Å and then etched in SF_6/Ar in a Plasma Therm reactive ion etch (RIE) system to create TLM patterns.^{14,15} The nitride samples were subsequently etched in $Cl_2/CH_4/H_2/Ar$ in an Electron Cyclotron Resonance (ECR) etcher to produce the mesas for the TLM patterns.¹⁶ The samples were annealed at temperatures from 300 to 900 °C for 15 sec under a nitrogen ambient in a RTA system (AG-410). Temperature dependent TLM measurements were made over the range -50 °C to 125 °C on the as-deposited and 900 °C (InGaN) and 500 °C (InN) annealed samples. These measurements make it possible to determine the dominant conduction mechanism over the barrier, and the results were compared to theoretical values. The error in

DISCLAIMER

**Portions of this document may be illegible
in electronic image products. Images are
produced from the best available original
document.**

DISCLAIMER

This report was prepared as an account of work sponsored by an agency of the United States Government. Neither the United States Government nor any agency thereof, nor any of their employees, make any warranty, express or implied, or assumes any legal liability or responsibility for the accuracy, completeness, or usefulness of any information, apparatus, product, or process disclosed, or represents that its use would not infringe privately owned rights. Reference herein to any specific commercial product, process, or service by trade name, trademark, manufacturer, or otherwise does not necessarily constitute or imply its endorsement, recommendation, or favoring by the United States Government or any agency thereof. The views and opinions of authors expressed herein do not necessarily state or reflect those of the United States Government or any agency thereof.

these measurements was estimated to be $\pm 10\%$ due mainly to geometrical contact size effects. The widths of the TLM pattern spacings varied slightly due to processing, (maximum of $\pm 5\%$) as determined by SEM measurements, which were taken into account when calculating the contact resistances.

RESULTS AND DISCUSSION

Figure 1 shows the theoretical curves for contacts to InGaN of this doping level exhibiting thermionic, thermionic field, or field emission as their dominant conduction mechanisms. The curves are shown only to give the expected temperature dependence of ρ_c and the magnitude of the specific contact resistance is arbitrary. The theoretical values are calculated from¹⁷

$$\rho_c \propto \exp(\Phi_b/E_{00}) \text{ for field emission} \quad (1)$$

$$\rho_c \propto \exp[\Phi_b/E_{00} \coth(qE_{00}/kT)] \text{ for thermionic field emission} \quad (2)$$

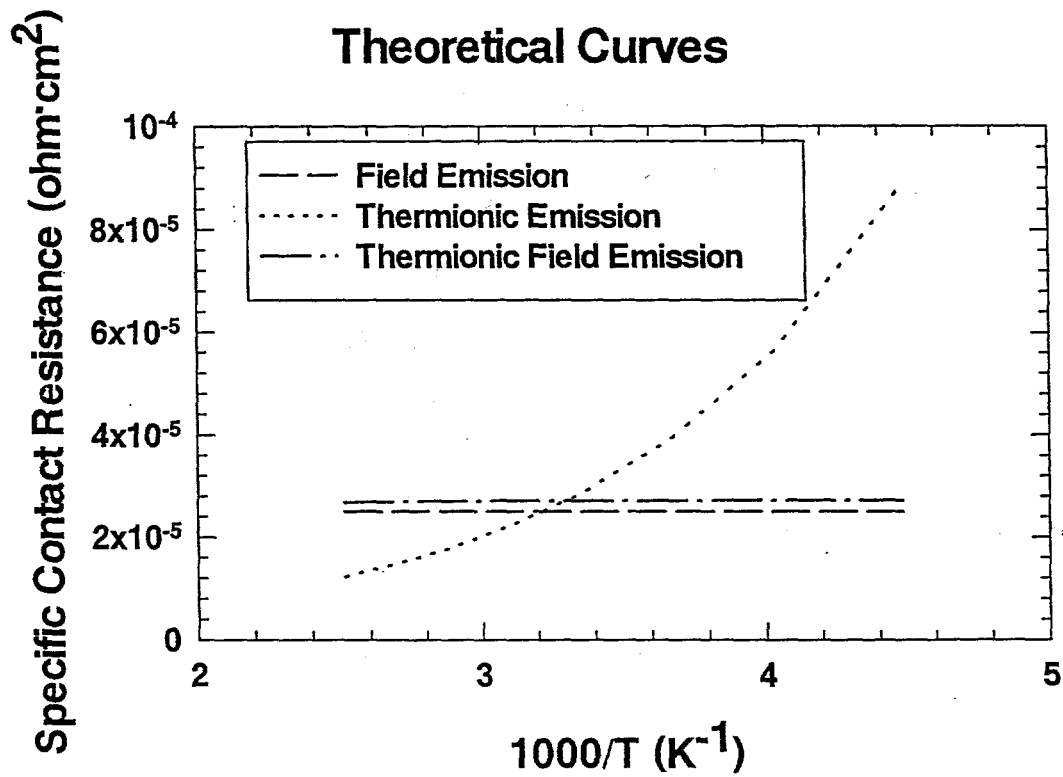


Figure 1. Theoretical curves for the temperature dependence of specific contact resistance of contacts in which thermionic emission, thermionic field emission, or field emission are the dominant conduction mechanism.

$$\varrho_c \propto \exp(q\Phi_b/kT) \text{ for thermionic emission} \quad (3)$$

where

$$E_{00} = h/4\pi[N_d/m^*\epsilon_s]^{1/2} \quad (4)$$

with Φ_b being the barrier height, N_d the donor concentration in the semiconductor, m^* the effective mass of electrons in the material and ϵ_s the permittivity of the semiconductor. For field emission $qE_{00}/kT \gg 1$, for thermionic field emission $qE_{00}/kT \sim 1$, and for thermionic emission $qE_{00}/kT \ll 1$, with $q/kT \approx 0.026$ eV at 300 K. A fixed barrier height (1 eV) was assumed for calculations of the three conduction mechanisms. As values have not been definitively established for m^* and ϵ_s for all the nitride compounds, the best available values for InN were used, ($m^* = 0.1m_e$ and $\epsilon_s = 8\epsilon_0$).¹⁸

Over the temperature range we studied there was little difference between the slope expected for the theoretical field emission and thermionic field emission plots (Figure 1). The thermionic field emission does have a slight upward slope with increasing reciprocal temperature, but it is less than the error found in the experimental measurements on the samples. By contrast, the thermionic emission case shows an obvious trend over the temperature range.

Temperature dependent contact resistance values for InGaN contacted with W and WSi_x are shown in Fig. 2. The specific contact resistance is very low ($< 10^{-5} \Omega \cdot cm^2$) for both

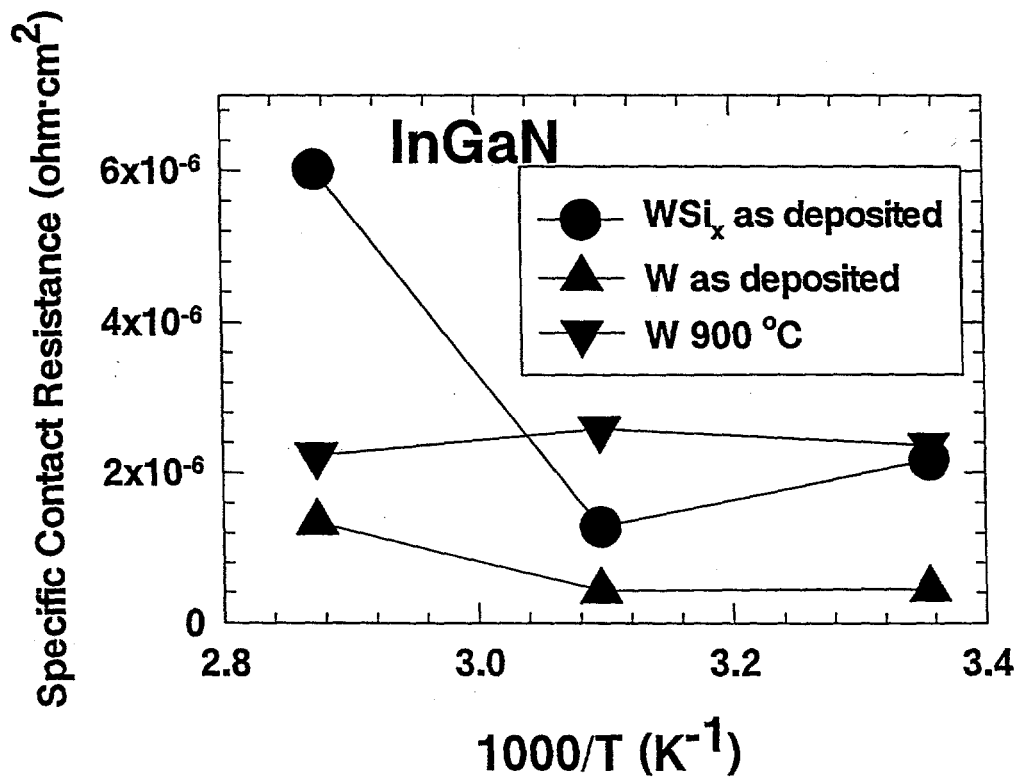


Figure 2. Experimentally measured, temperature-dependent specific contact resistance values for InGaN contacted with W and WSi_x .

metals. There is no clear pattern to the data over this temperature range. There is however no upward trend that would indicate thermionic emission. For this material, the value of E_{00} was estimated to be 0.63 eV based on doping levels. This gives a value of $qE_{00}/kT \sim 77$ indicating field emission conduction is expected to be dominant.

Figure 3 (top) shows the temperature dependent contact resistance data for InN contacted with WSi_x . The 500 °C annealed contact has approximately constant contact resistance over this temperature range, as is expected for InN with this doping level ($qE_{00}/kT \sim 24$).

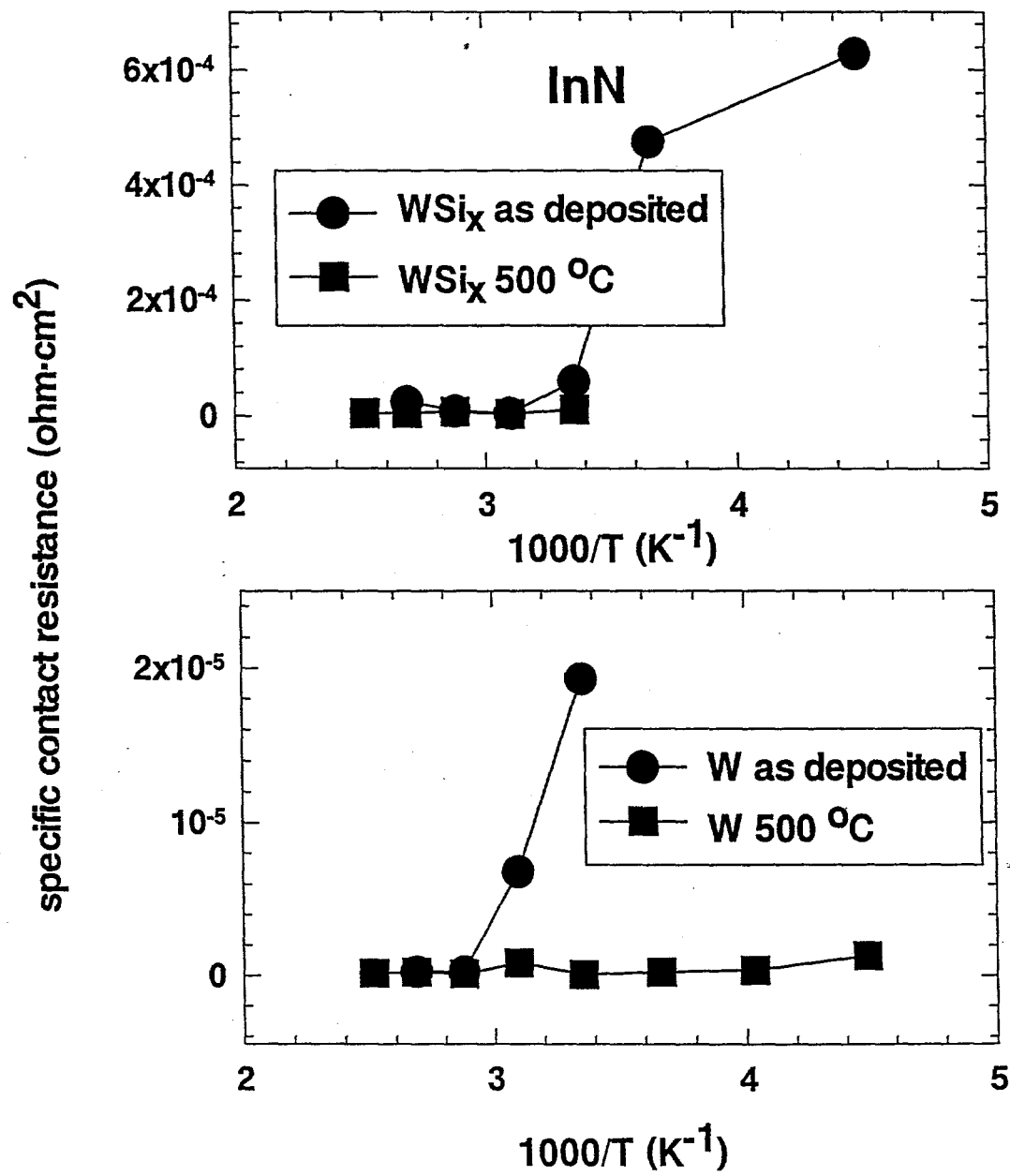


Figure 3. Experimentally determined, temperature-dependent specific contact resistance values for InN contacted with WSi_x and W.

The contact resistance for the as-deposited contact, however, rises with temperature, characteristic of thermionic emission. This may be a result of changing doping levels in the InN because of the sputter deposition of the contact, as is the case for GaAs. In comparing the data in Fig. 2 and 3 it is seen that contacts to InN are more sensitive to temperature than InGaN. The specific contact resistance of InN contacted with W as deposited and after a 500 °C anneal was also measured (Fig. 3, bottom). Again the annealed contact shows a relatively constant contact resistance over the range while the as-deposited contact shows an upward trend.

The contact resistance for W and WSi_x on InGaN as a function of subsequent annealing temperature is shown in Figure 4 (top). Both contacts had similar contact resistance as-deposited, $\sim 2-4 \times 10^{-7} \Omega \cdot cm^2$. Above 600 °C the WSi_x showed signs of degradation, with $Q_c \sim 10^{-5} \Omega \cdot cm^2$ at 900 °C. Q_c for the W contact sample dropped to $\sim 6 \times 10^{-8} \Omega \cdot cm^2$ at 600 °C and then increased slightly above that temperature. The contact resistances for ohmic contacts of W and WSi_x to InN as a function of annealing temperature are shown in Fig. 4 (bottom). As-deposited samples had similar contact resistances to InGaN, indicating a similar conduction mechanism. WSi_x contacts showed the most degradation at low annealing temperatures, with the resistance rising a factor of 5 after 300 °C annealing and then remaining constant. The W contacts began to degrade at 500 °C.

SUMMARY AND CONCLUSIONS

In summary, theoretical calculations based on the doping levels of InGaN and InN indicate that the dominant conduction mechanism in W-based ohmic contacts to these materials should be field emission. The experimental data fit curves for field emission or thermionic field emission for InGaN contacted with WSi_x and W. InN samples contacted with both W and WSi_x showed similar behavior after annealing at 500 °C, while for as-deposited the curves fit better to the thermionic emission case. This may indicate that the deposition of the contact metal lowered the doping levels in the InN, while annealing returned them to a higher level. W and WSi_x were found to produce low resistance ohmic contacts on n^+ InGaN and InN. W contacts proved to be the most stable, and also gave the lowest resistance to InGaN and InN, $Q_c < 10^{-7} \Omega \cdot cm^2$ after 600 °C anneal, and $1 \times 10^{-7} \Omega \cdot cm^2$ after 300 °C anneal, respectively.

ACKNOWLEDGMENTS

The work at Sandia is supported by DOE contract DE-AC04-94AL85000. The technical help of J. Escobedo, M.A. Cavaliere, D. Tibbets, G.M. Lopez, A.T. Ongstad, J. Eng and P.G. Glarborg at SNL is appreciated. The work at the UF is supported by DARPA (monitored by AFOSR, G.L. Witt), an AASERT grant through ARO (Dr. J. M. Zavada), and a University Research Initiative grant #N00014-92-J-1895 administered by AFOSR.

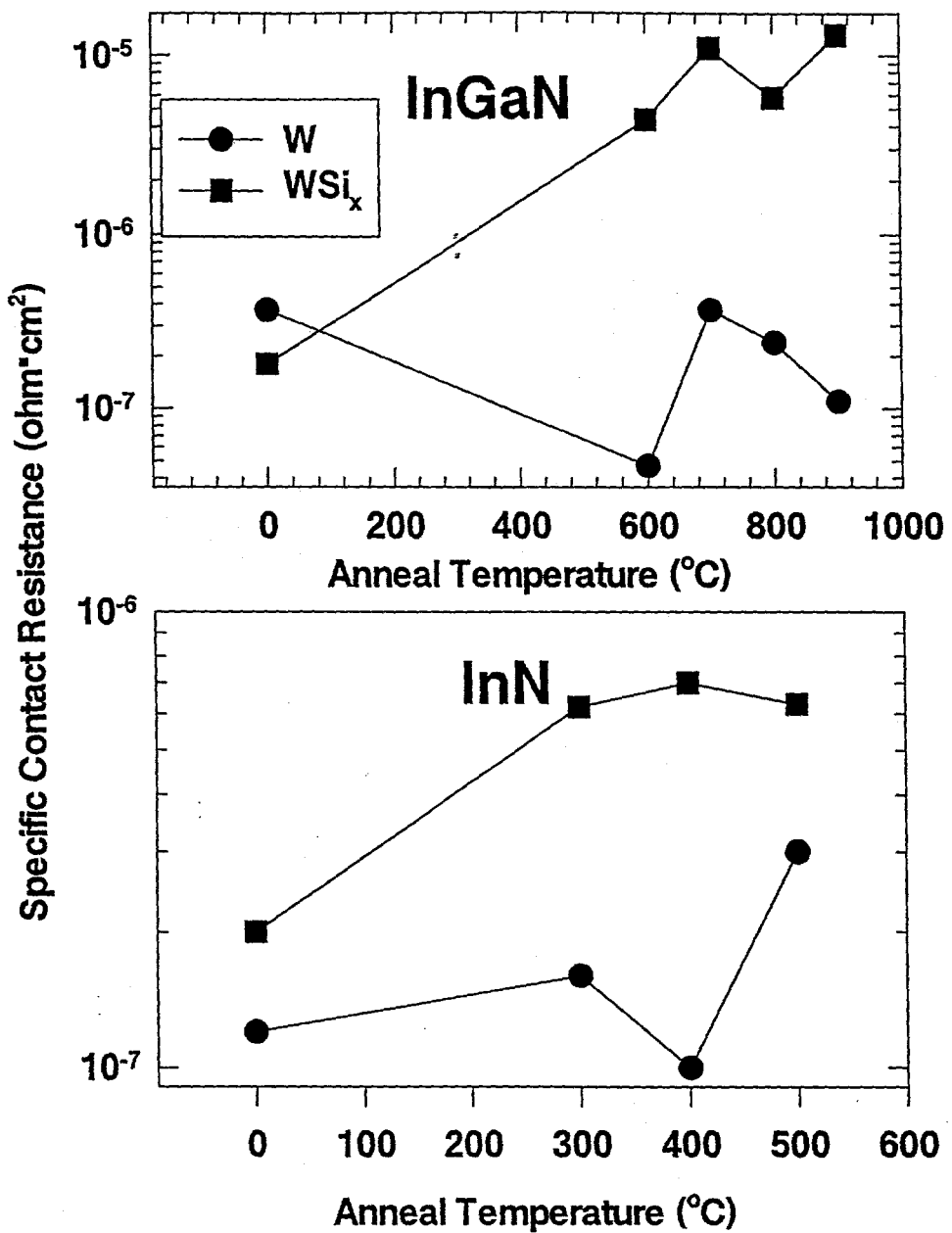


Figure 4. Specific contact resistance for W and WSi_x ohmic contacts to InGaN (top) and InN (bottom) as a function of annealing temperature.

REFERENCES

1. J.S. Foresi and T.D. Moustakas, *Appl. Phys. Lett.* **62** 2859 (1993).
2. M.A. Khan, T.N. Kuznia, A.R. Bhattacharya and D.T. Olson, *Appl. Phys. Lett.* **62** 1786 (1993).
3. S. Nakamura, T. Mukai and M. Senoh, *Jpn. J. Appl. Phys.* **30** L1998 (1991).

4. S.C. Binari, L.B. Rowland, W. Kruppa, G. Kelner, K. Doverspike and D.K Gaskill, Electron. Lett. **30** 1248 (1994).
5. S. Nakamura, M. Senoh and T. Mukai, Appl. Phys. Lett. **62** 2390 (1993).
6. M.E. Lin, Z. Ma, F.Y. Huang, Z.F. Fan, L.A. Allen and H. Morkoc, Appl. Phys. Lett. **64** 1003 (1994).
7. M.W. Cole, D.W. Eckart, T. Monahan, R.L. Pfeffer, W.Y. Han, F. Ren, C. Yuan, R.A. Stall, S.J. Pearton, Y. Li and Y. Lu, J. Appl. Phys. **80** 278 (1996).
8. M.E. Lin, F.Y. Huang and H. Morkoc, Appl. Phys. Lett. **64** 2557 (1994).
9. F. Ren, C.R. Abernathy, S.N.G. Chu, J.R. Lothian and S.J. Pearton, Appl. Phys. Lett. **66** 1503 (1995).
10. F. Ren, C.R. Abernathy, S.J. Pearton and P.W. Wisk, Appl. Phys. Lett. **64** 1508 (1994).
11. F. Ren, in GaN and Related Materials, ed. S.J. Pearton (Gordon and Breach, NY 1996).
12. C.R. Abernathy, J. Vac. Sci. Technol. A **11** 869 (1993).
- 13 C.R. Abernathy, Mat. Sci. Eng. Rep. **14**, 203 (1995).
14. R.J. Shul, D.J. Rieger, A.G. Baca, C. Constantine and C. Barratt, Electron. Lett. **30** 85 (1994).
15. R.J. Shul, M.E. Sherwin, A.G. Baca and D.J. Rieger, Electron. Lett. **32** 70 (1996).
16. R.J. Shul, S.P. Kilcoyne, M. Hagerott-Crawford, J.E. Parmeter, C.B. Vartuli, C.R. Abernathy and S.J. Pearton, Appl. Phys. Lett. **66** 1761 (1995).
17. A.Y.C. Yu, Solid State Electron, **13**, 239 (1970).
18. L.L. Smith and R.F. Davis, in Properties of Group III Nitrides, ed. J.H. Edgar, EMIS Datareview (INSPEC, London 1994).